McLafferty Rearrangement of the Radical Cations of Butanal and 3-Fluorobutanal: A Theoretical Investigation of the Concerted and Stepwise Mechanisms

DANIEL NORBERG, NESSIMA SALHI-BENACHENHOU
Department of Quantum Chemistry, Uppsala University, Box 518, 751 20 Uppsala, Sweden

Received 28 November 2006; Revised 13 May 2007; Accepted 28 May 2007
DOI 10.1002/jcc.20797
Published online 2 July 2007 in Wiley InterScience (www.interscience.wiley.com).

Abstract: The stepwise and concerted pathways for the McLafferty rearrangement of the radical cations of butanal (Bu^+) and 3-fluorobutanal (3F-Bu^+) are investigated with density functional theory (DFT) and *ab initio* methods in conjunction with the 6-311+G(d,p) basis set. A concerted transition structure (TS) for Bu^+, (**H**), is located with a Gibbs barrier height of 37.7 kcal/mol as computed with CCSD(T)//BHandHLYP. Three pathways for the stepwise rearrangement of Bu^+ have been located, which are all found to involve different complexes. The barrier height for the H_γ transfer is found to be 2.2 kcal/mol, while the two most favorable TSs for the C_α–C_β cleavage are located 8.9 and 9.2 kcal/mol higher. The energies of the 3F-Bu^+ system have been calculated with the promising hybrid meta-GGA MPWKCIS1K functional of DFT. Interestingly, the fluorine substitution yields a barrier height of only 20.5 kcal/mol for the concerted TS, (**3F-H**). A smaller computed dipole moment, 12.1 D, for (**3F-H**) compared with 103.2 D for (**H**) might explain the stabilization of the substituted TS. The H_γ transfer, with a barrier height of 4.9 kcal/mol, is found to be rate-determining for the stepwise McLafferty rearrangement of 3F-Bu^+, in contrast to the unsubstituted case. By inspection of the spin and charge distributions of the stationary points, it is noted that the bond cleavages in the concerted rearrangements are mainly of heterolytic nature, while those in the stepwise channels are found to be homolytic.

 J Comput Chem 29: 392–406, 2008

Key words: fragmentation; substitution effects; addition complex; electron spin resonance; hydrogen bonding

Introduction

The McLafferty rearrangement is a combined transfer of a γ-hydrogen (H_γ) to a double bonded atom through a six-membered transition state, and cleavage of the α–β bond (C_2–C_3 in Scheme 1) and takes place in radical cation compounds (for a review on McLafferty rearrangement reactions, see, e.g., ref. 1). The majority of experimental investigations on this rearrangement type are interpreted in terms of a stepwise mechanism (see, e.g., refs. 2–5, as well as ref. 6 and references therein) although some results pointed toward a concerted mechanism (see e.g. refs. 7 and 8). In particular, an extensive experimental investigation, utilizing both ^{13}C and ^{2}H kinetic isotope effects, clearly indicated that the McLafferty rearrangement of ketone radical cations is stepwise.[9] However, Stone et al.[7] proposed a concerted mechanism for the loss of acetaldehyde from the benzyl ethyl ether radical cation, which is also a McLafferty type reaction, in collisional activation spectra measurements. A few years later, the same group of authors[8] confirmed this observation by using Rice–Ramsperger–Kassel–Marcus (RRKM) theory on the same reaction. No evidence could be found for hydrogen scrambling in the elimination of acetaldehyde from the benzyl ethyl ether radical cation, which excludes the possibility for the reaction to occur in a stepwise manner via a distonic ion intermediate.

The stepwise or concerted nature of the McLafferty rearrangement has also been addressed in a number of theoretical investigations. Two contradictory studies appeared in 1968. Hence, using nonempirical MO calculations, Boer et al.[10] suggested a stepwise mechanism for the McLafferty rearrangement of the 2-pentanone radical cation, while Dougherty[11] argued that this type of reaction is electrocyclic, thus proceeding through a concerted transition structure (TS).

The butanal radical cation (Bu^+) is the one of the simplest compounds for modeling the McLafferty rearrangement and it has therefore been used extensively as a prototype for investigation of this fragmentation type. Hence, for the rearrangement of Bu^+ to the vinyl alcohol radical cation and ethylene

This article contains supplementary material available via the internet at http://www.interscience.wiley.com/jpages/0192-8651/suppmat

Correspondence to: N. Salhi-Benachenhou; e-mail: Nessima.Salhi@kvac.uu.se

(Scheme 1), Ha et al.[12] compared one stepwise pathway, which dissociates from a linear conformer of a distonic intermediate, with the concerted channel using geometries and energies optimized at the unrestricted HF/3-21G level* by constraining the TSs to planar C_S symmetry. Those calculations[12] supported a concerted mechanism for the rearrangement. On the basis of Ha's C_S symmetric concerted TS[12] and UHF/3-21G estimations of the energy of a symmetry unconstrained TS for decomposition of the distonic intermediate, Hudson et al.[13] performed RRKM calculations of the rates of the different mechanisms and concluded that the concerted pathway cannot compete with stepwise fragmentation. However, it was later shown[6,14] that the enforced C_S symmetry of Ha et al.[12] leads to stationary states having two imaginary vibrational frequencies and, thus, not to true TSs, which renders the results from the early studies[12,13] of doubtful value. Dorgio et al.[14] proceeded by computing fully optimized UHF/3-21G geometries for the stationary structures involved in the H_γ transfer step of the title rearrangement of Bu^+ with energies at the UMP2/6-31G* level. No concerted pathway was found in that study and the authors concluded[14] that "it seems unlikely that a concerted pathway could exist along with a stepwise one." This conclusion was substantiated by Liu and Pulay[6] who investigated the McLafferty rearrangement of Bu^+ with UMP2/6-31G*//UHF/4-31G. Neither in that study could a concerted TS be found. Instead, two stepwise pathways were located: C_2–C_3 bond cleavage either from the linear or from a cyclic conformer of the distonic intermediate.[6] To our knowledge, the most recent theoretical investigation of the McLafferty rearrangement was reported in 1992 by Trigueros et al.,[15] who also studied the Bu^+ system, using the semiempirical AM1 and MNDO methods for optimization of both geometries and energies. In that study, the authors presented concerted TSs at both levels and, furthermore, concluded[15] that this mechanism was favored over stepwise fragmentation. However, in the concerted TS,[15] the O—H_γ distance computed with MNDO (AM1) is 0.96 Å (0.99 Å), which is very similar to the O–H bond length of protonated formaldehyde[16] (0.98 Å). Since this fact indicates that the H_γ transfer is essentially complete in the semiempirically optimized TSs, these are most likely not associated with the concerted McLafferty rearrangement.

Hence, from the theoretical standpoint, the results from the studies of the McLafferty rearrangement of Bu^+ are inconclusive due to the lack of structural and energetic knowledge of the concerted TS. This is the missing key feature, which would complete the picture of the ground state potential energy surface (PES) for this model compound. Therefore, we decided to reinvestigate this reaction with emphasis on a thorough investigation of the region on the PES where a concerted H_γ transfer and C_2–C_3 bond cleavage can be expected to occur. Furthermore, while the previous studies have focused primarily on the energetic and structural factors governing the reaction, little attention has been paid to the underlying electronic structures and how these change during the course of the fragmentation. Therefore, we also present here an in-depth analysis of the rearrangement of the atomic spin and charge. For these purposes, we have investigated four reaction channels for the McLafferty fragmentation of Bu^+ to the vinyl alcohol radical cation and ethylene. The various reaction channels, together with all located stationary points[†] are displayed in Scheme 2. A second motive of this work is to expand the knowledge of aldehydic McLafferty rearrangement reactions beyond this well-studied model compound of Bu^+. A substituted Bu^+, the 3-fluorobutanal radical cation (3F-Bu^+), has been chosen for this purpose. This particular substitution is interesting since it might be expected to influence the properties of the steps involving cleavage of the C_2–C_3 bond. Furthermore, it has been shown both experimentally and computationally that the replacement of one of the H atoms in the methyl radical with CF_3 results in a destabilization of the formed $\bullet CH_2CF_3$ radical.[17] This suggests that fluorine atoms at position 3 in Bu^+ should exert a destabilizing effect on the distonic compounds formed after H_γ transfer and, consequently, raise the barrier for their formation, and possibly also favor a concerted rearrangement channel in which radical localization on C_4 is avoided. We have, therefore, also investigated the reaction channels for the McLafferty fragmentation of 3F-Bu^+ to the vinyl alcohol radical cation and fluoroethylene. In Scheme 3, the various channels of the substituted PES are presented, where the names of the stationary points are augmented with the prefix "3F-."

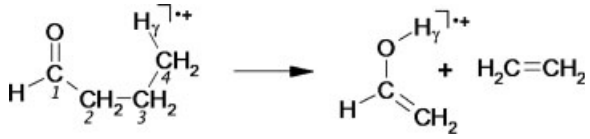

Scheme 1. McLafferty rearrangement of the butanal radical cation to the vinyl alcohol radical cation and ethylene.

Computational Details

The Gaussian03 suite of programs[18] has been used for all quantum chemical calculations and the abbreviations relating to the employed methods are taken from this program package. Molekel[19] was used for inspection of final geometries and vibrational frequencies and for making pictures of the optimized stationary structures. All quantum chemical calculations have been performed without symmetry constraints in the unrestricted formalism (restricted for ethylene and fluoroethylene) in conjunction with the 6-311+G(d,p) basis set using default convergence criterions. Unless necessary for the discussion, we disregard the prefix "U," which designates the unrestricted formalism, as well as the 6-311+G(d,p) basis set in the notation of the computational levels. The frozen-core approximation was used in all post-SCF computations. The production geometries for the stationary structures in both the Bu^+ and the 3F-Bu^+ systems have been optimized with MP2. Vibrational normal mode analysis and IRC calculations were employed for the characterization

*All abbreviations are explained in the *Computational Details* section.

†Following the notation of Liu and Pulay,[6] all of the optimized stationary structures, except for the two individual product species, are labeled with bold faced capital letters within parentheses.

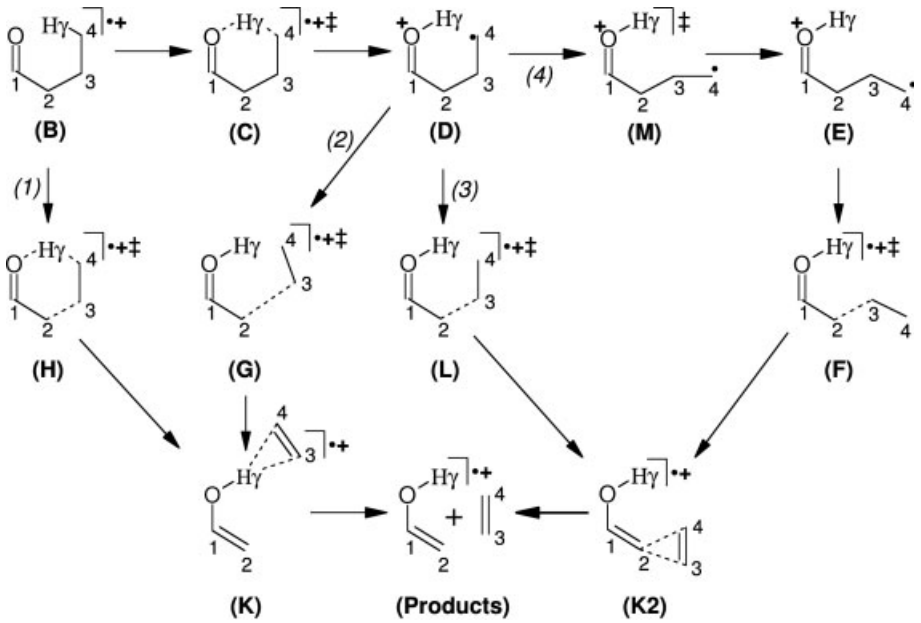

Scheme 2. Mechanisms of the McLafferty rearrangement of the butanal radical cation.

of the optimized stationary points. For comparison, we have also optimized all stationary points in the Bu^+ system with B3LYP and BHandHLYP. However, structures (**G**), (**H**), and (**3F-H**) could not be located at the MP2 level, instead their production geometries have been optimized with BHandHLYP. Electronic energies for the species in the Bu^+ system have been calculated with CCSD(T) while we have used the recently proposed[20] hybrid meta-GGA MPWKCIS1K[‡] functional of DFT for the compounds on the 3F-Bu^+ PES. Gibbs energies have been constructed by adding the electronic energies to the Gibbs thermal corrections at 298.15 K and 1.0 atm, which were computed using the unscaled MP2 frequencies [BHandHLYP for (**G**), (**H**), and (**3F-H**)]. We have not taken into account the effects of basis set superposition, since we are mainly interested in the isomerization channels leading to fragmentation rather than in the prediction of accurate overall reaction energetics.

Truhlar and coworkers found the MPWKCIS1K functional to be one of the top three candidates in a recent evaluation of a large number of DFT functionals for computing barrier heights, and this method was even shown to outperform QCISD for this purpose.[20] These authors compared the calculated barrier heights against best estimates of classical forward and reverse barrier heights for a large number of both hydrogen transfer and non-hydrogen transfer reactions. The mean-signed error and mean-unsigned-error for MPWKCIS1K were found to be 0.3 and 1.7 kcal/mol, respectively. In particular, this functional performed well for the fluorine containing reactions which were addressed.[20] Based on these promising results, we believe that MPWKCIS1K is a good choice of method since the present reactions involve both hydrogen transfer and non-hydrogen transfer steps. However, we also evaluated MPWKCIS1K by computing single-point energies with this method on the MP2 structures in the unsubstituted system and compared the resulting barrier heights with those predicted with CCSD(T). The resulting mean deviation and mean absolute deviation of the MPWKCIS1K computed barrier heights are found to be only −1.6 kcal/mol and 1.6 kcal/mol, respectively, consistent with the finding of Truhlar and coworkers.[20] A detailed description of our evaluation can be found in the Supporting Information.

It is well-known[21] that the results obtained from the UMP2 method should be viewed with precaution for calculations where the unrestricted reference wave-function suffers from spin-contamination. However, since the spin-contamination of the UMP2 wave-functions in the Bu^+ system are found to be rather modest for most structures, the largest value of $\langle S^2 \rangle$ being 0.860 for (**L**), these geometries are assumed to be of good quality. An overall low degree of UMP2 spin contamination is also noted in the substituted system, the largest value of $\langle S^2 \rangle$ being 0.894 for (**3F-L**).

The B3LYP method has proven highly successful for calculating proton hyperfine coupling constants (^{1}H hfccs) of organic radicals.[22–25] Therefore, we used this method for computing the ^{1}H hfccs, atomic charges, spin densities, and dipole moments of the MP2 structures. The atomic charges were computed by fitting the charges to the electrostatic potential according to the Merz–Singh–Kollman (MK) scheme[26] using default atomic radii for all atoms. Since the main positive charge is carried by the hydrogen atoms in the present species, we have summed the hydrogen atomic charges into their respective adjacent heavy atoms. The resulting charges are referred to as "group charges" throughout the text. For instance, the C_4 group charge refers to the MK atomic charge of C_4 plus the MK atomic charges of all hydrogens bound to C_4. A full description of the charge distributions is provided in the Supporting Information. Unless other-

[‡]Note that MPWKCIS1K is not a standard keyword of Gaussian03; the keyword specification for performing calculations in Gaussian03 at this level is: #MPWKCIS IOp(3/76 = 0590004100); see also ref. 20.

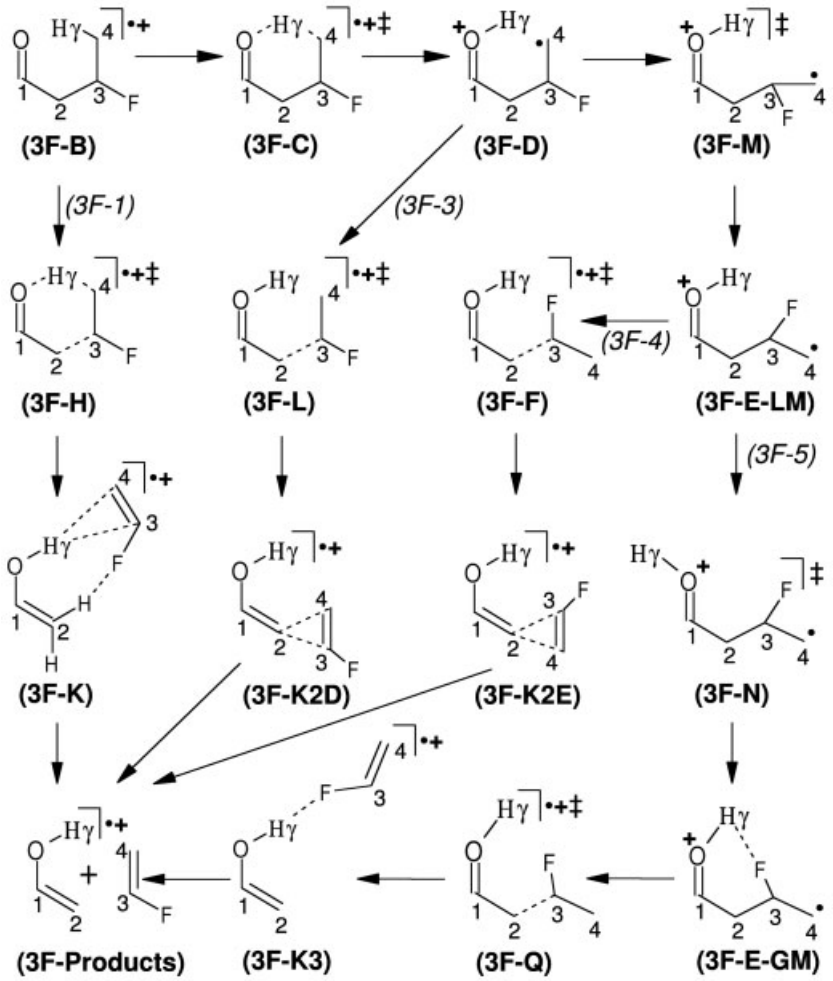

Scheme 3. Mechanisms of the McLafferty rearrangement of the 3-fluorobutanal radical cation.

wise noted, Gibbs energies, MP2 optimized geometries, and frequencies as well as B3LYP-computed dipole moments, charges, and spin densities are used in the discussion. For (**H**), (**G**), and (**3F-H**), BHandHLYP geometries and frequencies are employed.

Results and Discussion

McLafferty Rearrangement of the Butanal Radical Cation

In Scheme 2, the four channels of the McLafferty rearrangement of Bu^+ which have been located in the present work are a concerted mechanism; *(1)*: (**B**)–(**H**)–(**K**)–(**Products**), and three stepwise channels; *(2)*: (**B**)–(**C**)–(**D**)–(**G**)–(**K**)–(**Products**), *(3)*: (**B**)–(**C**)–(**D**)–(**L**)–(**K2**)–(**Products**), and *(4)*: (**B**)–(**C**)–(**D**)–(**M**)–(**E**)–(**F**)–(**K2**)–(**Products**), where (**Products**) refers to the vinyl alcohol radical cation and ethylene. In this work, the PES for the McLafferty rearrangement of Bu^+ is augmented with the *(1)* and *(2)* channels, while channels *(3)* and *(4)* have been partially investigated[6,13,14] with *ab initio* methods before. Structures (**B**), (**C**), (**D**), (**E**), (**L**), and (**F**) were previously discussed by Liu and Pulay,[6] while the notation (**H**) has been employed in several studies[6,12,13] for the concerted TS. In addition, four novel stationary points are here introduced: (**K**), (**K2**), (**M**), and (**G**). (**B**) is a cyclic conformer (C_1–C_2–C_3–C_4 = 301.2°) of ionized butanal. Besides, two linear conformers of ionized butanal have been found: (**A-GM**) and (**A-LM**) (C_1–C_2–C_3–C_4 = 179.0° and 180.0°, respectively). (**A-LM**) corresponds to the C_S symmetric structure (**A**) (with O–C_1–C_2–C_3 = 0.0°) studied by Liu and Pulay,[6] while (**A-GM**) is an asymmetric compound (with O–C_1–C_2–C_3 = 110.9°) located in the present work with a slightly lower energy (see Table 1 for the energies). (**D**) and (**E**) are the cyclic (C_1–C_2–C_3–C_4 = 305.2°) and linear (C_1–C_2–C_3–C_4 = 178.5°) conformers, respectively, of the distonic compound formed after H_γ transfer in the stepwise pathways, while (**K**) and (**K2**) are two weakly bounded complexes. As for the transition structures, (**C**) is the TS for the H_γ transfer in the stepwise pathways, (**M**) is the TS for interconversion of the distonic conformers while (**G**), (**L**), and (**F**) are three TSs for C_2–C_3 bond cleavage in the stepwise routes.

Table 1. Relative Energies (in kcal/mol) of the Stationary Structures Involved in the McLafferty Rearrangement of the Butanal Radical Cation.

	Optimization			Single-point at MP2 geometry				
	B3LYP	BHandHLYP	MP2	PMP2[a]	MPWKCIS1K	CCSD(T)	Gibbs[b]	ZPC[c]
Local minima								
(**A-LM**)	3.5	0.9	0.4	0.5	1.3	1.0	1.0	0.2
(**A-GM**)	2.4	0.1	−0.8	−0.7	0.3	−0.2	0.2	0.5
(**B**)	0.0	0.0	0.0	0.0	0.0	0.0	0.0	0.0
(**D**)	0.3	−5.9	−13.7	−12.0	−5.5	−4.5	−2.5	1.3
(**E**)	2.3	−1.5	−8.3	−6.8	−1.4	0.8	1.6	1.2
(**K**)	8.6	5.3	0.3	1.4	7.8	8.3	5.8	−0.9
(**K2**)	5.5	–[f]	1.5	3.3	8.0	10.6	11.0	1.3
(**Products**)[d]	21.8	18.2	15.1	16.6	20.6	22.0	9.6	−1.8
Transition structures								
(**C**)	3.0	3.1	2.5	2.2	1.1	2.4	2.2	−1.2
(**M**)	3.9	0.3	−6.5	−5.0	0.4	2.5	3.9	1.1
(**G**)	12.5	10.7	8.7[e,f]	9.0[e]	12.3[e]	15.1[e]	14.4[b]	0.7[c]
(**L**)	5.9	–[f]	4.2	2.6	7.6	10.8	11.1	0.7
(**F**)	5.6	–[f]	4.0	2.7	7.6	10.7	11.4	1.0
(**H**)	–[g]	34.7	40.9[e,g]	36.2[e]	36.4[e]	39.9[e]	37.7[b]	−2.0[c]

The energy of **(B)** is taken as zero. All calculations have been done employing the 6-311+G(d,p) basis set.
[a]Spin-projected MP2 energies.
[b]The Gibbs energy is constructed by adding the CCSD(T) computed electronic energy with the thermal correction to Gibbs energy calculated from unscaled frequencies at the MP2/6-311+G(d,p) level (BHandHLYP/6-311+G(d,p) for **(G)** and **(H)**) at 298.15 K and 1.0 atm.
[c]Zero-point vibrational energy correction (ZPC) computed from unscaled frequencies at the MP2/6-311+G(d,p) level (BHandHLYP/6-311+G(d,p) for **(G)** and **(H)**), relative to **(B)**.
[d]This is the sum of the energies taken from separate calculations on ethylene and the vinyl alcohol radical cation.
[e]Single-point calculation on the BHandHLYP-optimized geometry.
[f]The stationary structure has not been found at this level of theory.
[g]The concerted TS does not exist at the B3LYP and MP2 levels (see the text for further discussion on this matter).

Optimized Stationary Points

The MP2-optimized structures of the local minima (**A-LM**), (**A-GM**), (**B**), (**D**), (**E**), (**K**), (**K2**), vinyl alcohol radical cation, and ethylene are displayed in Figure 1a with selected geometrical parameters.

All the local minima have been optimized with MP2, B3LYP, and BHandHLYP, except for (**K2**), which was not located with BHandHLYP. Comparing B3LYP and BHandHLYP with the MP2-optimized geometries for the minima, a closer agreement between BHandHLYP and the latter method is found, in general. This is reflected by the fact that the maximum absolute deviations between MP2 and B3LYP [BHandHLYP] in all minima for covalent bond lengths, bond angles, and dihedral angles are 0.075 Å for C_2-C_3 in (**E**) [0.020 Å for C_3-C_4 in (**K**)], 7.9° for C_2-C_1-H in (**A-LM**) [3.0° for C_1-O-H in (**D**)], and 40.2° for $C_1-C_2-C_3-C_4$ in (**K2**) [6.4° for $O-C_1-C_2-H_{2a}$ in (**B**)], respectively.

The MP2-optimized transition structures [BHandHLYP for (**G**) and (**H**)] are displayed in Figure 1b with selected geometrical parameters and imaginary frequencies. Transition structures (**C**) and (**M**) have been located at all levels of theory, while (**L**) and (**F**) have not been found with BHandHLYP. Comparing the B3LYP and BHandHLYP with the MP2-optimized geometries for the TSs, it is noted that MP2 predicts the earliest TS for the H_γ transfer in the stepwise route, while B3LYP gives the latest TS for this reaction step. This is reflected by the optimized $O—H_\gamma$ (C_4–H_γ) distance in (**C**), which is 1.665 Å (1.149 Å) and 1.286 Å (1.323 Å) for MP2 and B3LYP, respectively. On the contrary, the C_2-C_3 distance in TSs (**L**) and (**F**) (see Scheme 2) are found with B3LYP to be 0.056 and 0.063 Å shorter than the corresponding MP2 distance of 2.265 and 2.320 Å, respectively. Thus, B3LYP predicts the earliest TSs for these transformations. Finally, a third TS, (**G**), for the C_2–C_3 cleavage in the stepwise route has been located in the present study, which connects (**D**) to complex (**K**). The C_2–C_3 distance of (**G**) is found to be very large, 3.238 Å (3.120 Å) with B3LYP (BHandHLYP), which shows that (**G**) is a much later TS than the abovementioned (**L**) and (**F**) TSs.

The concerted TS, (**H**), connecting (**B**) to complex (**K**) (Scheme 2), has been located with BHandHLYP but has not been found with B3LYP and MP2. By inspection of the reaction path for the concerted rearrangement, it is noted that the main geometrical change from (**B**) to (**H**) is an elongation of C_2–C_3 from 1.525 to 2.692 Å, while the H_γ transfer starts very near the TS region, as reflected by the C_4–H_γ distances of 1.098 and 1.130 Å in the minima and the TS, respectively. This fact renders the concerted channel highly asynchronous. The facts that (**H**) could not be found by us using B3LYP and MP2 and that

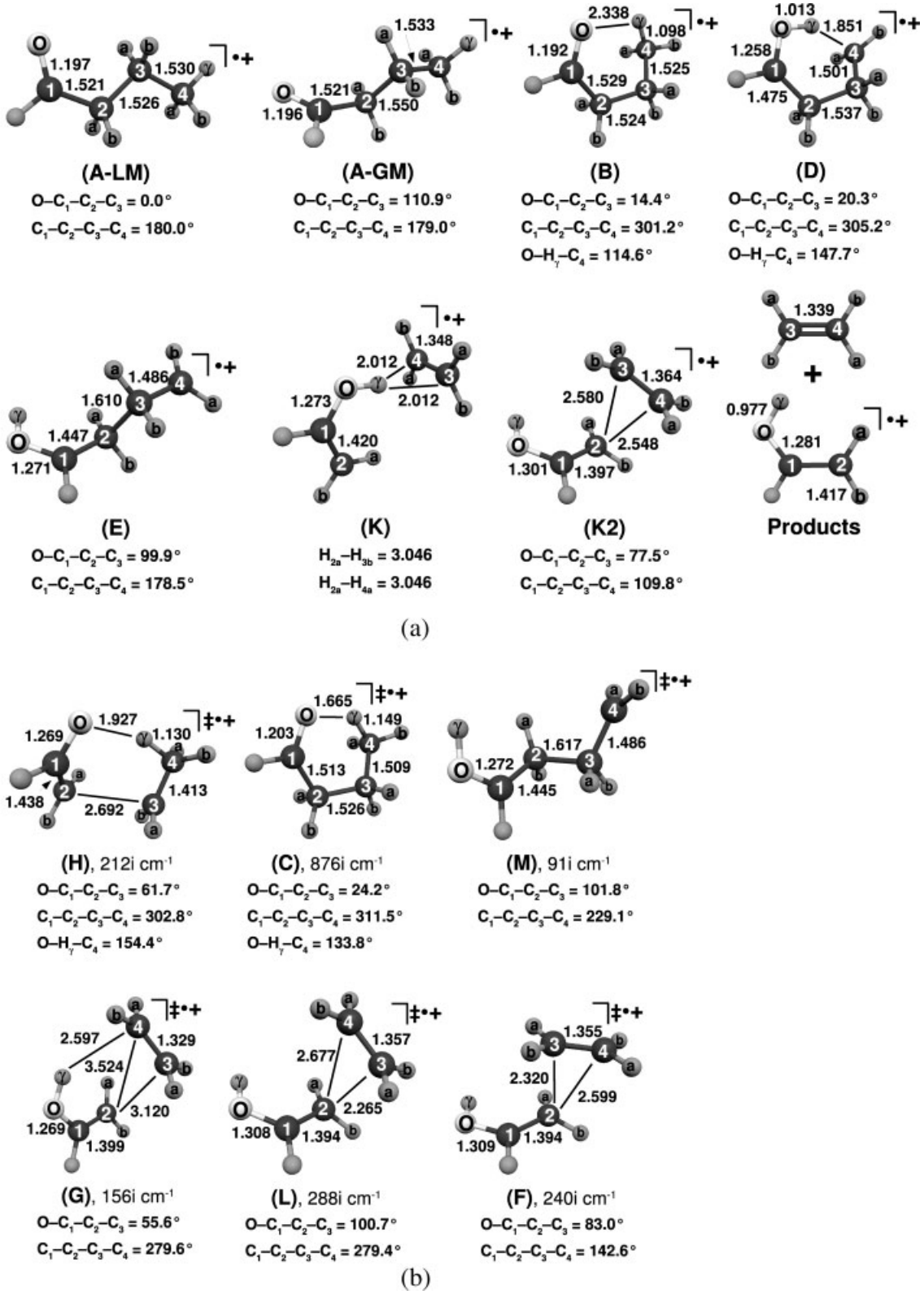

Figure 1. (a) MP2/6-311+G(d,p)-optimized geometries of the local minima for the McLafferty rearrangement of the butanal radical cation. Structures (**A-LM**) and (**A-GM**) are linear conformers of the butanal radical cation and do not explicitly take part in the rearrangement. When (**K2**) is formed from TS (**L**) (see Scheme 2 and Fig. 1b), labels 3 and 4 should be interchanged and O–C_1–C_2–C_3 and C_1–C_2–C_3–C_4 are in that case 107.6° and 283.5°, respectively, for (**K2**). Bond lengths are given in Ångström. (b) MP2/6-311+G(d,p) optimized geometries and imaginary frequencies [BHandHLYP/6-311+G(d,p) for (**G**) and (**H**)] of the transition structures for the McLafferty rearrangement of the butanal radical cation. Bond lengths are given in Ångström.

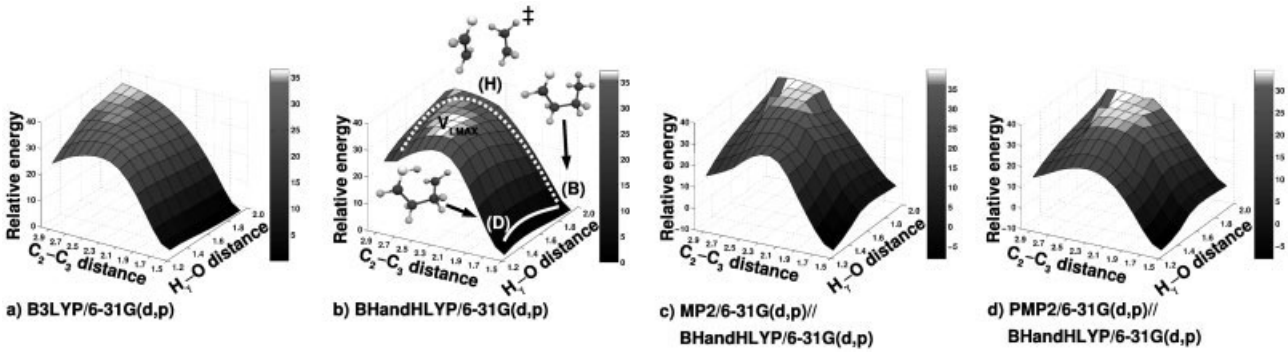

Figure 2. Two-dimensional energy profiles of the potential energy surface region for concerted rearrangement of Bu+ at the various levels of theory. In Figure 2b, the concerted and the stepwise channels are highlighted with dotted and solid lines, respectively. Distances are in Ångström and energies in kcal/mol.

the previous[6,14] *ab initio* studies of the McLafferty rearrangement of Bu^+ also failed to locate (**H**) motivated us to perform an extensive investigation of the region of the PES where the concerted isomerization could be expected to occur. For this purpose, 2-dimensional energy surface scans were performed at the B3LYP and BHandHLYP levels of theory in conjunction with the 6-31G(d,p) basis set. Both scans were started from (**B**) optimized with B3LYP/6-31G(d,p), in which the O–H_γ and C_2–C_3 distances are 1.952 and 1.527 Å, respectively. From these values, the O–H_γ distance was decreased, incrementally by 0.1 Å, to a final value of 1.252 Å and for each O–H_γ distance, C_2–C_3 was increased to 2.927 Å, using the same incremental stepsize. All other degrees of freedom were allowed to relax during each optimization step. The resulting B3LYP and BHandHLYP energy profiles are displayed in Figures 2a and 2b, respectively. By inspection of these profiles, the cause of the failure to locate (**H**) with B3LYP becomes obvious. In order for the concerted TS to exist, there must be a local energy maximum on the PES, which separates the concerted and stepwise pathways. As is clear from Figure 2a, no such maximum is found. The point of highest energy on this energy profile is found at maximum O–H_γ and C_2–C_3 distances and the surface goes downhill in all directions moving toward lower values of these parameters. On the other hand, Figure 2b explains the success of the BHandHLYP method to locate (**H**) since on this energy profile, the necessary local maximum (V_{LMAX} in Fig. 2b) does exist. Thus, increasing the amount of HF exchange included in the DFT functional from 20 to 50% makes the concerted TS to appear on the PES. Next, the MP2 and spin-projected MP2 (PMP2) methods were addressed. Because of the increased amount of CPU time needed for performing a corresponding scan with MP2, single-point calculations at this level using the 6-31G(d,p) basis set were performed at the converged structures in the BHandHLYP 2D-scan. The resulting energy profiles[§] for MP2 and PMP2 are shown in Figures 2c and 2d, respectively. As was noted for B3LYP, it is obvious that energy valleys for concerted rearrangement are missing on both these surfaces, which explains why (**H**) cannot be located at the MP2 level. Furthermore, and in agreement with the topologies of Figures 2a and 2c, all attempts of optimizing (**H**) with B3LYP and MP2 in conjunction with the larger 6-311+G(d,p) basis set collapsed to TSs involved in the stepwise rearrangement, suggesting that the failure of these methods to locate a concerted TS for the present rearrangement is inherent to the methods themselves.[¶] Finally, the BHandHLYP/6-311+G(d,p)-optimized value of 1.927 Å for the O–H_γ distance in (**H**) (see also Fig. 1b) together with the topologies of the energy profiles in Figures 2a–2d assert that, if a TS for concerted rearrangement of Bu^+ does exist, the O–H_γ distance in this structure would be about 2 Å. Based on this fact, it can be concluded that the previously AM1- and MNDO-optimized concerted TSs[15], with O–H_γ = 0.99 and 0.96 Å, respectively, can most likely not be associated with the concerted McLafferty rearrangement of Bu^+.

Rearrangement Mechanisms

Gibbs energy profiles for the four McLafferty rearrangement channels leading from (**B**) to fragmentation into (**Products**) are displayed in Figure 3, while the energies relative to (**B**) of the stationary structures from all levels of theory employed in the present work are reported in Table 1. Table 2 displays the calculated group charges, atomic spin densities of the heavy atoms, and dipole moments of all stationary points in Figure 3.

As can be noted in Figure 3, the barrier height for the concerted rearrangement is predicted to be very large, 37.7 kcal/mol, a fact which is also reproduced with all the methods

[§]An inspection of the MP2//BHandHLYP and PMP2//BHandHLYP energy profiles (Figs. 2c and 2d) reveals that they are not as smooth as those in Figs. 2a and 2b. This may be due to the fact that no geometry optimization was performed for any point on the former.

[¶]To further assess the reliability of the BHandHLYP prediction, (**H**) was also optimized with MPWKCIS1K, which, indeed, also converged to a TS for concerted rearrangement, with very similar geometrical parameters. The equivalence of the two geometries of (**H**) becomes obvious by inspection of the critical distances of the breaking and forming bonds. Thus, the BHandHLYP (MPWKCIS1K)-computed O–H_γ, C_4–H_γ, and C_2–C_3 distances in (**H**) are 1.927 Å (1.825 Å), 1.130 Å (1.144 Å), and 2.692 Å (2.642 Å), respectively (see also Fig. 1b).

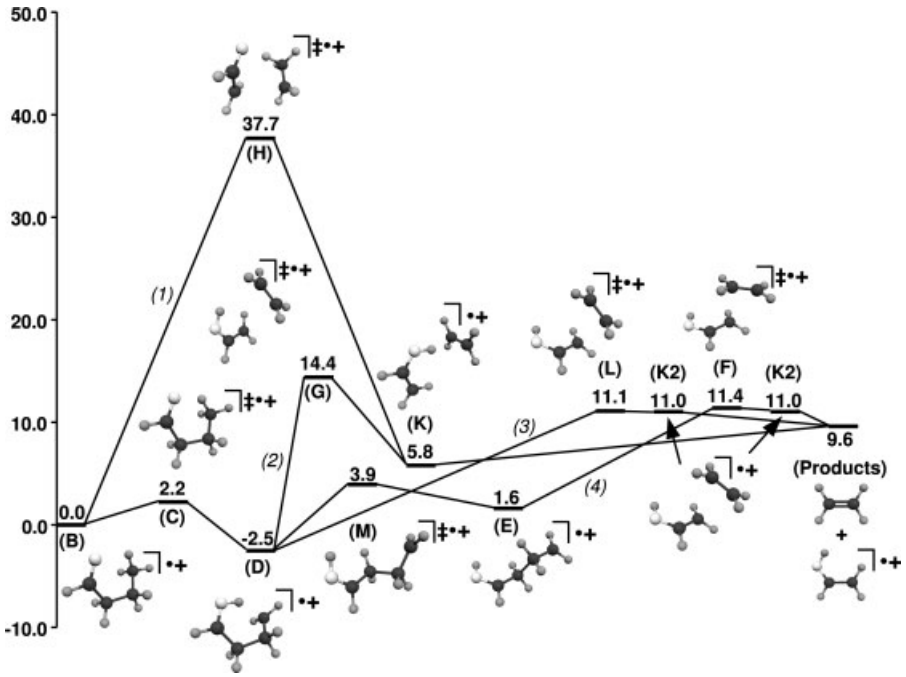

Figure 3. CCSD(T)//MP2 (CCSD(T)//BHandHLYP for (**G**) and (**H**)) Gibbs energy profiles (in kcal/mol) for the concerted and stepwise McLafferty rearrangement of the butanal radical cation. All calculations have been done employing the 6-311+G(d,p) basis set.

(Table 1). A rationalization of the high energy of (**H**) might be the substantial increase noted in the dipole moment when this structure is approached. Hence, proceeding from (**B**) to (**H**), the computed dipole moment changes from 5.6 D to 103.2 D, indicating that an unfavorable[27] charge separation is built up in the concerted TS. Once the complex (**K**) is formed, the dipole moment gets smaller again: 5.0 D. An inspection of the group charges in Table 2 shows, indeed, that a charge separation is built up in (**H**). This is reflected by the fact that the C_1 and O group charges decrease from 0.6 to 0.5 and −0.1 to −0.3, respectively, during the uphill transformation. Simultaneously, the C_3 and C_4 group charges in the ethylene fragment increase from 0.3 to 0.4 and 0.1 to 0.3, respectively. Hence, a net positive charge of 0.3 is transferred into the ethylene fragment when going from (**B**) to (**H**) creating a separation of positive and negative charge in (**H**), which should be unfavorable in gas phase. It is also noted that, in the downhill conversion to (**K**), the positive charge is transferred back into the vinyl alcohol fragment as is reflected by the fact that the C_3 and C_4 group charges decrease to 0.1 in (**K**) and further to 0.0 in (**Products**). In addition, Table 2 reveals that during the conversion of (**B**) to (**H**), the atomic spin density on C_2 (O) increases (decreases) from 0.1 (0.6) to 0.7 (0.3) while the spin densities on the other atoms are essentially unaltered. For the following transformation to (**K**), the spin density on C_2 (O) increases (decreases) further to 0.8 (0.2). Furthermore, the C_3 and C_4 atomic spin densities in the ethylene fragment remain close to zero during the (**B**)−(**H**)−(**K**) rearrangement. Based on these facts, and because the positive charge flows into the ethylene fragment in (**H**) while it is transferred back to the vinyl alcohol fragment in (**K**), the C_2–C_3 and C_4−H_γ bond cleavages can be characterized as being *heterolytic* in the concerted channel.

The H_γ transfer reaction in the stepwise route is, on the other hand, accompanied by homolytic cleavage of the C_4–H_γ bond

Table 2. B3LYP/6-311+G(d,p)//MP2/6-311+G(d,p)-Computed Group Charges, Atomic Spin Densities of the Heavy Atoms, and Dipole Moments μ (in Debye) for the Stationary Structures Involved in the McLafferty Rearrangement of the Butanal Radical Cation [Except for (**A-LM**) and (**A-GM**)].

	Group charges					Atomic spin densities					
	C1	C2	C3	C4	O	C1	C2	C3	C4	O	μ
Local minima											
(**B**)	0.6	0.1	0.3	0.1	−0.1	0.0	0.1	0.0	0.0	0.6	5.6
(**D**)	0.6	0.0	0.3	0.0	0.1	0.0	0.0	−0.1	0.9	0.0	5.3
(**E**)	0.5	0.0	0.3	0.1	0.1	0.1	0.0	−0.1	1.0	0.0	5.8
(**K**)	0.5	0.2	0.1	0.1	0.1	0.1	0.8	0.0	0.0	0.2	5.0
(**K2**)	0.5	0.0	0.2	0.2	0.0	0.3	0.3	0.2	0.2	0.1	7.6
(**Products**)	0.6	0.3	0.0	0.0	0.2	0.1	0.7	0.0	0.0	0.2	7.4[a]
Transition structures											
(**C**)	0.6	0.1	0.3	0.2	−0.1	0.0	0.1	0.0	0.2	0.5	5.5
(**M**)	0.6	−0.1	0.3	0.0	0.1	0.1	0.0	−0.1	1.0	0.0	5.6
(**G**)	0.5	0.2	0.1	0.2	0.1	0.2	0.6	0.0	0.2	0.2	5.6
(**L**)	0.5	0.0	0.2	0.2	0.0	0.3	0.3	0.0	0.4	0.1	101.1
(**F**)	0.5	0.0	0.2	0.2	0.0	0.3	0.3	0.0	0.4	0.1	8.0
(**H**)	0.5	0.1	0.4	0.3	−0.3	−0.1	0.7	0.1	0.0	0.3	103.2

[a]This is the dipole moment of the vinyl alcohol radical cation. Ethylene has no dipole moment.

and this H_γ transfer is therefore a migration of a hydrogen atom. This is reflected by the fact that the atomic spin density on C_4 (O) increases (decreases) from 0.0 (0.6) in (**B**) to 0.2 (0.5) in (**C**), and further to 0.9 (0.0) in (**D**) (Table 2). Since the positive charge in (**D**) resides mainly on the C_1 (0.6) and the C_3 (0.3) groups, the compound is confirmed to be distonic. Consistent with the previous calculations,[6,14] this reaction step has a low barrier height (2.2 kcal/mol), and gives support for rapid formation of distonic intermediates in McLafferty rearrangement reactions.

However, the H_γ transfer is here found much less exothermic, only −2.5 kcal/mol, than reported[6] previously. That is, Liu and Pulay calculated an MP2/6-31G*//HF/4-31G reaction energy of −10.3 kcal/mol (−9.4 kcal/mol after spin projection) for this step.[6] Our calculations show that MP2 (PMP2) yields a reaction energy of −13.7 kcal/mol (−12.0 kcal/mol) while the predictions of BHandHLYP and MPWKCIS1K//MP2, −5.9 and −5.5 kcal/mol, respectively, are close to CCSD(T)//MP2: −4.5 kcal/mol (see also Table 1). Hence, the MP2 method seems to overstabilize distonic (**D**) compared to our best computations. An inspection of the magnitudes of $\langle S^2 \rangle$ for (**B**) (0.779) and (**D**) (0.762) shows that the spin contamination is low and also of similar magnitudes in both structures and this may therefore not be the cause of this discrepancy.

Proceeding to the C_2–C_3 bond cleavage, three channels emerge from (**D**). In paths *(2)* and *(3)*, the bond is broken directly while following path *(4)* requires initial rearrangement to (**E**). Path *(2)* proceeds through TS (**G**) to complex (**K**) with a barrier of 16.9 kcal/mol (Fig. 3). This complex may be characterized as an *ion-molecule* complex (or *ion-neutral* complex), since its spin density and charge are mainly located on the vinyl alcohol fragment and are distributed as in (**Products**) (Table 2). Table 2 reveals further that the atomic spin density on C_2 (C_4) increases (decreases) from 0.0 (0.9) in (**D**) to 0.6 (0.2) in (**G**) and further to 0.8 (0.0) in (**K**), while it increases on the oxygen atom from 0.0 in (**D**) to 0.2 in (**G**) and (**K**). This implies, as expected, that the C−C bond cleavage is homolytic and that one electron from the C_2–C_3 bond in (**D**) combines with the single electron on C_4 and forms the doubly occupied π orbital in ethylene, while the other electron delocalizes over the π system in the vinyl alcohol fragment. Interestingly, recent infrared action spectroscopy measurement[28] for the addition of the hydroxyl radical to acetylene, complemented with high-level *ab initio* calculations, suggested that a preactivation complex, similar to (**K**), stabilized by an interaction between the hydrogen of the OH radical and the π-orbitals of acetylene, exists as a shallow intermediate in this addition process.[28**] This fact, combined with the rather large reverse barrier to (**D**), 8.6 kcal/mol, indicates that (**K**) might be experimentally detectable. Finally, despite the fact that the Gibbs thermal correction to the CCSD(T) energy lowers the relative energy of (**Products**) by 12.4 kcal/mol due to a favorable entropy effect, complex (**K**) is still more stable than the products on the Gibbs energy scale (see Table 1).

The other channel, path *(3)*, in which the C_2–C_3 bond in (**D**) is directly broken, proceeds through TS (**L**) with a barrier height of 13.6 kcal/mol, which is lower than that of path *(2)* (Fig. 3). This step was previously[6] assumed to lead to dissociation but is here found to connect to a second complex (**K2**) (Fig. 1a). As was the case in path *(2)*, the total fragmentation of (**D**) to (**Products**) involves a net homolytic C_2–C_3 bond cleavage. Despite this overall behavior, the electronic rearrangement in path *(3)* differs from the former channel as can be seen in Table 2. During the conversion of (**D**) to (**L**), the atomic spin density on C_4 is reduced from 0.9 to 0.4, while it increases from 0.0 to 0.3 on both C_1 and C_2. Thus, as expected, the spin density is transferred from the ethylene fragment to the vinyl alcohol fragment. On the other hand, the downhill progression to (**K2**) involves only an equilibration of spin density over the C_3 and C_4 atoms and no spin redistributions in the vinyl alcohol fragment. Furthermore, the positive charge in the ethylene fragment in (**K2**) is large as reflected by C_3 and C_4 group charges of 0.2. Hence, the ethylene fragment in (**K2**) has net spin and positive charge of 0.4, suggesting that this complex might not properly be called an ion-molecule complex. Hence, in path *(3)*, the total spin transfer is not completed until the radical species has dissociated, while in path *(2)*, it is complete already at the formation of complex (**K**). A final issue on path *(3)* needs to be addressed. Table 2 shows that the majority of compounds have dipole moments in the range 5.0–8.0 D. However, the dipole moment of (**L**), 101.1 D, is predicted to be almost as large as that of (**H**) (103.2 D) even though the energy of the former TS is much lower (−26.6 kcal/mol) than that of the latter. This discrepancy, together with the fact that a dipole moment of only 7.6 D is predicted for (**K2**), prompted us to compute also the dipole moments of all compounds using the MP2 densities. The resulting dipole moments can be found in the Supporting Information available for this work. It is found, indeed, that the magnitudes of the MP2 dipole moments are very similar to those in Table 2 and, in particular, the MP2-computed dipole moments of (**L**) and (**H**), 101.1 D and 103.3 D, respectively, are very close to those predicted with B3LYP. While the large dipole moment computed for the TS (**H**) may be rationalized by its large energy, as discussed above, no explanation could be found for the unusually large dipole moment predicted for TS (**L**).

In the final stepwise path *(4)*, which also leads to cleavage of the C_2–C_3 bond, distonic (**D**) first rearranges to the linear conformer (**E**) through a low barrier: 6.4 kcal/mol for TS (**M**). Table 2 shows that the distonic character is preserved during this conversion. Because (**D**) is found to lie 4.1 kcal/mol below (**E**), the linear conformer is the least stable distonic minimum. The C_2–C_3 bond cleavage in this channel proceeds from (**E**), through TS (**F**), with a barrier height of 9.8 kcal/mol. Also (**F**) is here found to connect to complex (**K2**) and the total reaction step is characterized by the same spin and charge redistribution as was noted for path *(3)* (Table 2).

Furthermore, ion-molecule complexes stabilized by a H-bond–π-type interaction were located with MP2/6-31+G(d) by Selçuki and Aviyente[29] for the addition of the hydroxyl radical to the double bond in ethene, propene, and *cis*- and *trans*-2-butene. Comparing the distances between the hydrogen atom in the hydroxyl radical and the carbon atoms in ethene (2.510 Å) with the C_3–H_γ and C_4–H_γ distances found in (K**) (2.012 Å, see Fig. 1a), the present ion-molecule complex can be concluded to be much more tightly bound than the former.

It is noted from Figure 3 that (**K2**) has essentially the same relative energy (11.0 kcal/mol) as (**L**) and (**F**) (11.1 and 11.4 kcal/mol, respectively). Hence, the reverse reactions back to the distonic structures (**D**) and (**E**) should proceed very easily. Moreover, it is also noted from Figure 3 that (**Products**) are located 1.4 kcal/mol below (**K2**) indicating that the complex is unstable in forward direction as well. Because of these facts, complex (**K2**) is probably better viewed as a common intersection for direct fragmentation of the distonic intermediates, rather than as a stable entity on the PES.

From the above analysis of the different channels leading to McLafferty rearrangement of Bu^+, it is concluded that the stepwise paths *(3)* and *(4)* constitute the most plausible mechanisms for the McLafferty rearrangement of Bu^+ in the gas phase because the relative energies of their critical TSs, (**L**) and (**F**), are found to be 11.1 and 11.4 kcal/mol, respectively, as compared to 14.4 kcal/mol for TS (**G**) in the stepwise path *(2)* and 37.7 kcal/mol for the concerted TS (**H**) in path *(1)*. It should be mentioned that, at the temperature (298.15 K) and pressure (1.0 atm) used in the Gibbs energy calculations, the equilibrium population is shifted very much toward the bound compound. A further study on the effects of different temperatures and pressures on the free energy profiles of the presented mechanisms could therefore be motivated.

Calculated ESR Parameters

The fact that the calculations show that the cyclic distonic species (**D**) is more stable than the linear conformer (**E**) (Table 1) is actually in disagreement with an ESR investigation[30] of ionized butanal in 2,4,6-tri-*tert*-butylnitrosobenzene (BNB) at 77 K. The product ESR spectrum gave major ^{1}H hfccs of 18.2 G for two H atoms and the authors concluded that these arise from a distonic adduct formed by the solvent and the solute.[30] Table 3 displays the computed ^{1}H hfccs for the most stable bound species (**A-GM**), (**B**), (**D**), and (**E**) together with experimental values. An inspection of this table shows that structure (**E**) is the only compound that has got two equivalent H atoms (H_{4a} and H_{4b}), with hfccs (−19.9 G and −19.8 G) in very good agreement with those measured[30] in the ESR experiment. Hence, the computed hfccs support the experimental suggestion[30] of a distonic adduct, but the experiment is in disagreement with the fact that (**D**) is the distonic compound with the lowest energy. One explanation for this discrepancy between theory and experiment is that the linear structure (**E**) might be more reactive with the BNB environment, or that cyclic (**D**) indeed reacts with the environment but transforms into a linear distonic adduct in a second step.

Table 3. B3LYP/6-311+G(d,p)-Computed ^{1}H hfccs (in Gauss) for the MP2/6-311+G(d,p)-Optimized Structures (**A-GM**), (**B**), (**D**), and (**E**) *Versus* Experimental Values.

Atom	(**A-GM**)	(**B**)	(**D**)	(**E**)	Exp[30]
H_1	95.0	110.1	6.1	−3.3	–
H_{2a}	−4.2	0.8	−0.1	0.1	–
H_{2b}	5.0	−1.4	−0.5	2.6	–
H_{3a}	1.8	42.7	55.9	7.8	–
H_{3b}	−0.3	3.7	7.2	11.4	–
H_{4a}	0.2	0.7	−12.8	−19.9	18.2
H_{4b}	−1.0	13.8	−15.7	−19.8	18.2
$H\gamma$	19.7	38.2	−2.7	−0.6	–

McLafferty Rearrangement of the 3-Fluorobutanal Radical Cation

The substituted isomer of ionized butanal addressed in this work was created by exchanging the hydrogen atom H_{3b} with an F atom (see compound (**B**) in Fig. 1a for the labels). The mechanisms of the McLafferty rearrangement of 3F-Bu^+ investigated here are schematically displayed in Scheme 3. One concerted channel, *(3F-1)*: (**3F-B**)–(**3F-H**)–(**3F-K**)–(**3F-Products**) was located, as were three stepwise pathways, *(3F-3)*: (**3F-B**)–(**3F-C**)–(**3F-D**)–(**3F-L**)–(**3F-K2D**)–(**3F-Products**), *(3F-4)*: (**3F-B**)–(**3F-C**)–(**3F-D**)–(**3F-M**)–(**3F-E-LM**)–(**3F-F**)–(**3F-K2E**)–(**3F-Products**), and *(3F-5)*: (**3F-B**)–(**3F-C**)–(**3F-D**)–(**3F-M**)–(**3F-E-LM**)–(**3F-N**)–(**3F-E-GM**)–(**3F-Q**)–(**3F-K3**)–(**3F-Products**). The names of the stationary points and paths on the substituted PES are chosen to be consistent with those on the PES of Bu^+. Thus, (**3F-B**) corresponds to substituted (**B**) and path *(3F-1)* is the substituted analog of channel *(1)* and so forth (see further Schemes 2 and 3). No substituted path corresponding to channel *(2)* has been found since the substituted TS corresponding to (**G**) was not located. Because of the lower symmetry of fluoroethylene compared to ethylene, the difference between *(3F-3)* and *(3)* on the one hand, and between *(3F-4)* and *(4)* on the other hand, is that the complex (**K2**), which is a common stationary point in the unsubstituted channels, is replaced by two distinct structures: (**3F-K2D**) and (**3F-K2E**) for the substituted paths *(3F-3)* and *(3F-4)*, respectively (Scheme 3). Path *(3F-5)* emerges as a new channel from (**3F-E-LM**), which corresponds to (**E**) in the unsubstituted case, due to the possibility of hydrogen bonding between the F atom and the O–H_γ moiety. Thus, (**3F-E-GM**) is formed from (**3F-E-LM**) via internal rotation about the C_1–C_2 bond through TS (**3F-N**), and (**3F-K3**) is a complex created through TS (**3F-Q**) when the C_2–C_3 bond in (**3F-E-GM**) is broken.

Comparison of the Optimized Stationary Points in the Bu^+ and 3F-Bu^+ Systems

The MP2-optimized minima involved in the McLafferty rearrangement of the 3F-Bu^+ are displayed in Figure 4a with selected geometrical parameters. In general, the F atom induces only minor changes in the length of most covalent bonds in the minima, which have unsubstituted counterparts. This is displayed by the mean deviation and mean absolute deviation of −0.001 Å and 0.012 Å, respectively, as computed from differences in covalent bond lengths between the substituted compounds and the parent unsubstituted species. However, a large structural change is noted for the complex (**3F-K**). This structure is tilted away from C_S symmetry as reflected, for instance, by the fact that the C_1–C_2–C_3–C_4 (C_1–C_2–C_4–C_3) dihedral angle is −87.2° (87.2°) in (**K**) and −63.0° (113.3°) in (**3F-K**). The geometrical change is driven by a favorable interaction between the F atom and the hydrogen atom H_{2a}, which is most easily appreciated by

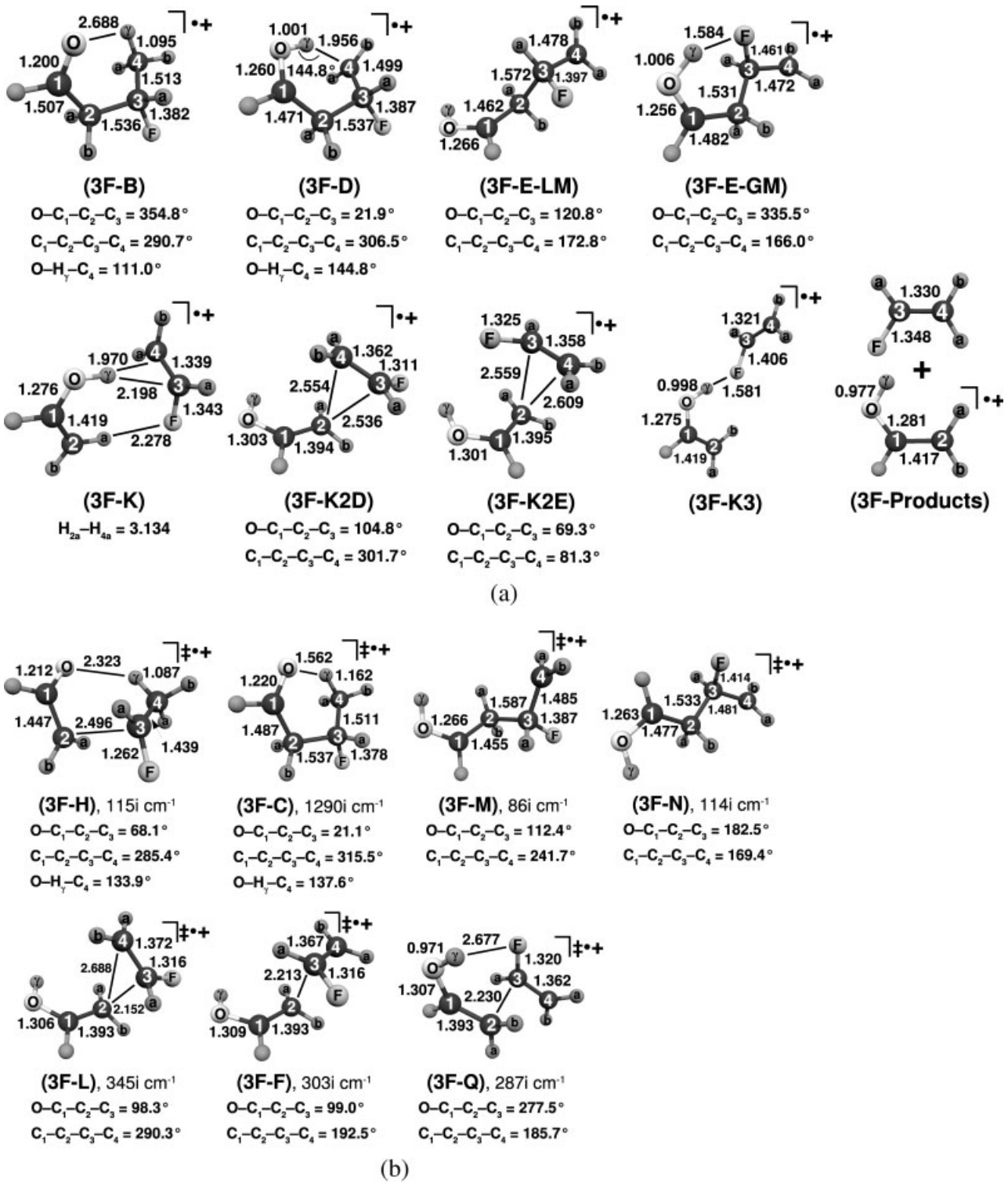

Figure 4. (a) MP2/6-311+G(d,p)-optimized geometries of the local minima for the McLafferty rearrangement of the 3-fluorobutanal radical cation. Bond lengths are given in Ångström. (b) MP2/6-311+G(d,p) optimized geometries and imaginary frequencies [BHandHLYP/6-311+G(d,p) for (**3F-H**)] of the transition structures for the McLafferty rearrangement of the 3-fluorobutanal radical cation. Bond lengths are given in Ångström.

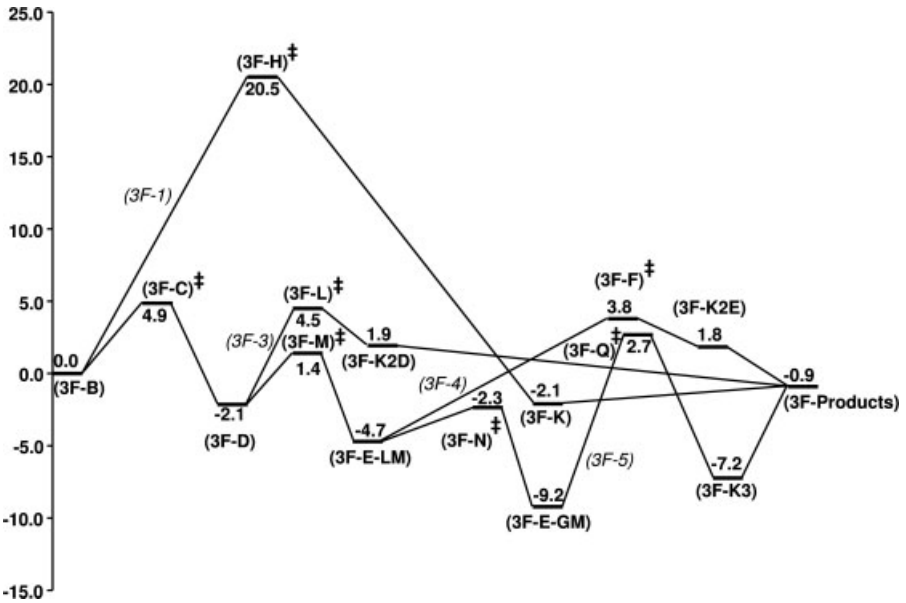

Figure 5. MPWKCIS1K//MP2 [MPWKCIS1K//BHandHLYP for (**3F-H**)] Gibbs energy profiles (in kcal/mol) for the concerted and stepwise McLafferty rearrangement of the 3-fluorobutanal radical cation. All calculations have been done employing the 6-311+G(d,p) basis set.

the fact that $H_{2a}-H_{3b} = H_{2a}-H_{4a} = 3.046$ Å in (**K**) (Fig. 1a), while $H_{2a}-F = 2.278$ Å and $H_{2a}-H_{4a} = 3.134$ Å in (**3F-K**) (Fig. 4a). Some important differences of interfragment distances in the Bu^+ and the 3F-Bu^+ systems are noted. In (**3F-B**), O–H_γ is predicted to be 2.688 Å, which is 0.350 Å longer than in (**B**), indicating that the substituted species should be less susceptible to H_γ transfer. Furthermore, C_4–H_γ in (**3F-D**) is increased, by 0.105 Å to 1.956 Å compared to (**D**), suggesting that also the reverse H_γ transfer should be less favorable in the substituted compound.

The MP2-optimized transition structures [BHandHLYP for (**3F-H**)] involved in the McLafferty rearrangement of the 3F-Bu^+ are displayed in Figure 4b with selected geometrical parameters and imaginary frequencies. Consistent with the long interfragment O–H_γ distance noted above for (**3F-B**), the substituted TS for H_γ transfer from this compound is later than its unsubstituted counterpart. This is reflected by the C_4–H_γ (O–H_γ) distance, which is 1.162 Å (1.562 Å) in (**3F-C**) and 1.149 Å (1.665 Å) in (**C**) (see Figs. 4b and 1b, respectively). On the contrary, the two TSs (**3F-L**) and (**3F-F**) for C_2–C_3 bond cleavage are earlier than their unsubstituted counterparts as the C_2–C_3 distance in these species are 2.152 and 2.213 Å, respectively, which is 0.113 Å and 0.107 Å shorter than in (**L**) and (**F**), respectively. A large structural change is also noted for the concerted TS (**3F-H**). From Figures 1b and 4b, it can be deduced that this TS becomes much earlier with respect to the C_2–C_3 bond cleavage, since this partial bond is shortened from 2.692 Å in (**H**) to 2.496 Å in (**3F-H**). On the other hand, the computed C_4–H_γ and O–H_γ distances of 1.087 and 2.323 Å, respectively, indicate that the substituted concerted rearrangement is even more asynchronous than its unsubstituted counterpart. Thus, from a structural point of view, the hydrogen transfer seems less favorable while the likelihood of C_2–C_3 bond cleavage increases in the substituted system compared to the unsubstituted system.

The Stationary Points (3F-E-GM), (3F-K3), (3F-N), and (3F-Q)

The linear structure (**3F-E-GM**) (C_1–C_2–C_3–$C_4 = 166.0°$) is formed from (**3F-E-LM**) via TS (**3F-N**) by internal rotation about the C_1–C_2 bond. As expected, the hydrogen bond F–H_γ (1.584 Å) in (**3F-E-GM**) is created at the expense of a weakening of the C_3–F bond, which is elongated with 0.064 Å in (**3F-E-GM**) compared to (**3F-E-LM**). On the other hand, the C_2–C_3 bond is significantly strengthened in (**3F-E-GM**) decreasing to 1.531 Å, from 1.572 Å in (**3F-E-LM**), indicating that the hydrogen-bonded compound is less susceptible for C_2–C_3 bond cleavage. An inspection of the geometry of complex (**3F-K3**), which is formed from (**3F-E-GM**) through TS (**3F-Q**) reveals that this species is also stabilized by hydrogen bonding, with F–H_γ = 1.581 Å. Interestingly, the IRC path for this reaction shows that the hydrogen bond is broken in the TS ($F-H_\gamma = 2.677$ Å), and is reformed in the complex.

Rearrangement Mechanisms

Gibbs energy profiles for the four McLafferty rearrangement paths, leading from (**3F-B**) to fragmentation into the vinyl alcohol radical cation and fluoroethylene, are displayed in Figure 5. The analysis of the spin and charge distributions of the structures in these channels reveals that paths *(3F-1)*, *(3F-3)*, and *(3F-4)* correspond closely to the unsubstituted paths *(1)*, *(3)*, and *(4)*, respectively. Hence, only the spin and charge redistribution of the unique path *(3F-5)* will be ironed out in detail here. An

inspection of Figure 5 reveals that the present substitution has a large impact on the barrier for the concerted H_γ transfer and C_2–C_3 bond cleavage. Thus, the barrier height for TS (**3F-H**) is predicted to be only 20.5 kcal/mol, which is 17.2 kcal/mol lower than that for the unsubstituted compound.[††] The facts that the C_2–C_3 bond cleavage is the most important structural parameter in the uphill path of the concerted rearrangement and, as noted above, that this bond is much shorter (-0.196 Å) in (**3F-H**) than in (**H**), might provide one explanation for the lower barrier height of the substituted species. A second, presumably more important, explanation is provided from the computed dipole moment of (**3F-H**). For the substituted species, the dipole moment is 12.1 D, which should be compared to the very large dipole moment computed for (**H**): 103.2 D. The dipole moments of all other substituted compounds range from 1.6 to 8.3 D indicating that this particular substitution has the largest impact on the dipole moment of the concerted TS. This suggests that the charge separation is substantially reduced in (**3F-H**) compared to (**H**), which should make the substituted concerted TS more favorable in the gas phase. Prompted by the stabilizing effect exerted by the F atom on the concerted TS, we also investigated the doubly substituted compound for this channel (both H atoms at C_3 are substituted with F atoms). However, the resulting barrier height is found to be 21.3 kcal/mol, indicating that no further stabilization of the concerted TS has occurred.

The activation energy for the H_γ transfer in the stepwise route increases upon substitution to 4.9 kcal/mol, a result which is consistent with the longer O–H_γ distance noted above for (**3F-B**) compared to (**B**). The thereby formed distonic species (**3F-D**) is located −2.1 kcal/mol below (**3F-B**), which yields this step slightly less exothermic than on the unsubstituted PES. The C_2-C_3 bond cleavage in path *(3F-3)* proceeds through TS (**3F-L**), which connects (**3F-D**) to complex (**3F-K2D**), with a forward (reverse) barrier of 6.6 kcal/mol (2.5 kcal/mol). Thus, it is noted that the forward barrier is lowered by 7.0 kcal/mol upon substitution and, moreover, that (**3F-K2D**) is more stable toward the reverse reaction than (**K2**) (see also Fig. 3).

Both of the *(3F-4)* and *(3F-5)* paths requires that (**3F-D**) rearranges to the linear distonic conformer (**3F-E-LM**). This reaction proceeds with a forward (reverse) barrier of 3.5 kcal/mol (6.1 kcal/mol) through TS (**3F-M**) (Fig. 5). Hence, in sharp contrast to the unsubstituted case, (**3F-E-LM**) is predicted to be more stable than the cyclic (**3F-D**). The C_2-C_3 bond cleavage in path *(3F-4)* proceeds through TS (**3F-F**), which connects (**3F-E-LM**) to complex (**3F-K2E**), with a forward (reverse) barrier of 8.5 kcal/mol (2.0 kcal/mol). Again the substituted complex is found to be more stable than (**K2**).

In the final path located on the substituted PES, *(3F-5)*, the hydrogen-bonded structure (**3F-E-GM**) is formed by internal rotation about C_1–C_2 in (**3F-E-LM**) through TS (**3F-N**) with low activation energy: 2.4 kcal/mol. An inspection of the atomic spin densities (1.0 on C_4 and 0.0 for the other atoms) and the group charges (0.0 on C_4) reveals that the distonic character is preserved in (**3F-E-GM**). The hydrogen bond in (**3F-E-GM**) stabilizes this species significantly and renders it the most stable isomer on the substituted PES with an energy of −9.2 kcal/mol relative to (**3F-B**) (see Fig. 5). In the second step of path *(3F-5)*, the C_2–C_3 bond is broken. This reaction proceeds through TS (**3F-Q**), which connects (**3F-E-GM**) to complex (**3F-K3**), with a forward (reverse) barrier of 11.9 kcal/mol (9.9 kcal/mol). Interestingly, the influence of the hydrogen bond in (**3F-K3**) is substantial and makes this complex the second most stable species on the substituted PES. Moreover, the large reverse barrier and the fact that (**3F-K3**) is located 6.1 kcal/mol below (**3F-Products**) indicate that this complex might be an important stationary point in the McLafferty rearrangement of 3F-Bu^+. As in the case of the unsubstituted complex (**K**), complex (**3F-K3**) is found to be more stable than the products despite the favorable entropy effect provided by the final dissociation to (**3F-Products**). It is noted for the (**3F-E-GM**)−(**3F-K3**) conversion that, on the uphill path, the atomic spin density on C_4 decreases to 0.5 and that it increases on C_1, C_2, and O to 0.2, 0.2, and 0.1, respectively. At the same time, the spin density on C_3 stays zero. In fact, this redistribution of spin resembles closely that found for the uphill paths of the C_2–C_3 bond cleavage steps in the unsubstituted channels *(3)* and *(4)*. However, the remaining spin density is transferred from the fluoroethylene fragment to the vinyl alcohol fragment during the downhill progression to the complex (**3F-K3**). Thus, the electronic rearrangement accompanying the C_2–C_3 bond cleavage in path *(3F-5)* occurs in a single step, which differs from the two unsubstituted channels.

From the above analysis of the different McLafferty rearrangement channels of 3F-Bu^+, it is concluded that the barrier height for the concerted path, 20.5 kcal/mol, is much lower than in the unsubstituted system (Table 1). The relative energies of the three substituted TSs for C_2–C_3 bond cleavage in the stepwise routes are located, successively, 4.5, 3.8, and 2.7 kcal/mol above (**3F-B**) (see Fig. 5). Since these energies are all lower than that for H_γ transfer, 4.9 kcal/mol, the H_γ transfer step is predicted to be rate-determining of the substituted reaction. Finally, despite the fact that the concerted rearrangement most likely cannot compete with stepwise fragmentation neither for the substituted species, the lowering of its barrier upon substitution is dramatic and might motivate a further study on the effects of other substituents on this barrier.

Conclusions

The concerted and stepwise mechanisms for the McLafferty rearrangement of the radical cations of butanal (Bu^+) and 3-fluorobutanal (3F-Bu^+) have been investigated using the 6-311+G(d,p) basis set.

At the CCSD(T) level, the lowest Gibbs energy pathways found for fragmentation of Bu^+ are the two stepwise channels displayed in Figure 6. The rate of fragmentation via both these paths are determined by the transition structures (TSs) (**L**) and (**F**) for cleavage of the C_α–C_β bond with energies of 11.1 and 11.4 kcal/mol, respectively, relative to the cyclic conformer (**B**) of Bu^+. The activation energy of the H_γ transfer is found to be

[††]It should be noted that the MPWKCIS1K Gibbs energies for the unsubstituted system collected in the supporting information also support a dramatic stabilization of the substituted concerted TS (15.2 kcal/mol).

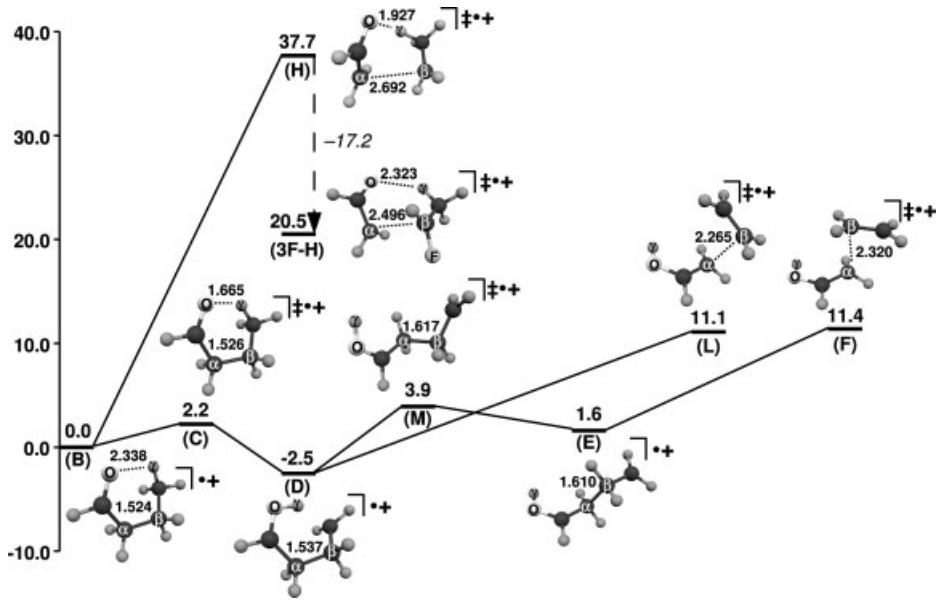

Figure 6. Gibbs energy profile displaying the concerted channel and the two lowest energy stepwise pathways for the McLafferty rearrangement of Bu^+. In addition, the profile shows the substantial stabilization of the concerted TS when a fluorine atom is substituted on C_β. Distances are in Ångström and energies are in kcal/mol.

much lower: 2.2 kcal/mol. In addition, a third stepwise channel has been located, which proceeds through a TS for C_α–C_β bond cleavage having a relative energy of 14.4 kcal/mol. It is found that all the stepwise routes connect to complexes before dissociation (not displayed in Fig. 6). In contrast to the stepwise channels, the concerted rearrangement of Bu^+, proceeding through TS (**H**), is found to have a much larger barrier, 37.7 kcal/mol, showing definitively that concerted H_γ transfer and C_α–C_β bond cleavage cannot compete with stepwise rearrangement for this compound (Fig. 6). One explanation for the high energy of the TS for the concerted rearrangement, (**H**), might be the unusually large dipole moment, which is predicted for this species: 103.3 D and 103.2 D with B3LYP//BHandHLYP and MP2//BHandHLYP, respectively. This suggests that an unfavorable charge separation is built up in the concerted TS, a conclusion that is supported by calculated atomic charges for the stationary points showing that a large amount of positive charge is being transferred to the ethylene fragment during the conversion from (**B**) to (**H**).

Interestingly, the fluorine substitution on C_β lowers the barrier height for the concerted TS (**3F-H**) to only 20.5 kcal/mol as computed with MPWKCIS1K (Fig. 6). The significantly lower energy of (**3F-H**) compared to (**H**) might be explained by its computed dipole moment, 12.1 D, which indicates that the unfavorable charge separation is removed upon substitution. Three pathways for stepwise McLafferty rearrangement have been located also for 3F-Bu^+. In contrast to the unsubtituted case, the H_γ transfer is predicted to be the rate-determining step of all these channels, with a computed activation energy of 4.9 kcal/mol. The relative energies of the three TSs for C_α–C_β bond cleavage in the substituted compound are predicted to be successively 2.7, 3.8, and 4.5 kcal/mol. Hence, despite the substantially lower barrier for the concerted substituted pathway, this channel is not competitive with stepwise fragmentation neither with this particular substitution.

Acknowledgments

We thank the Swedish National Supercomputer Center (NSC) for generous allocation of computer time. The authors thank Prof. O. Matsson, Prof. S. Lunell, and Mr. O. Anders Borg for helpful discussions.

References

1. Kingston, D. G. I.; Bursey, J. T.; Bursey, M. M. Chem Rev 1974, 74, 215.
2. Wesdemiotis, C.; Feng, R.; McLafferty, F. W. J Am Chem Soc 1985, 107, 715.
3. Tureček, F.; Drinkwater, D. E.; McLafferty, F. W. J Am Chem Soc 1990, 112, 993.
4. Osterhold, T. H.; Brauman J. I. J Am Chem Soc 1990, 112, 2014.
5. Nibbering, N. M. N. J Am Soc Mass Spectrom 2004, 15, 956.
6. Liu, R.; Pulay, P. J Comput Chem 1992, 13, 183.
7. Stone, D. J. M.; Bowie, J. H.; Underwood, D. J. J Am Chem Soc 1983, 105, 1688.
8. Allison, C. E.; Stringer, M. B.; Bowie, J. H.; Derrick, P. J. J Am Chem Soc 1988, 110, 6291.
9. Stringer, M. B.; Underwood, D. J.; Bowie, J. H.; Allison, C. E.; Donchi, K. F.; Derrick, P. J. Org Mass Spectrom 1992, 27, 270.
10. Boer, F. P.; Shannon, T. W.; McLafferty, F. W. J Am Chem Soc 1968, 90, 7239.
11. Dougherty, R. C. J Am Chem Soc 1968, 90, 5788.
12. Ha, T.-K.; Radloff, C.; Nguyen, M. T. J Phys Chem 1986, 90, 2991.
13. Hudson, C. E.; Griffin, L. L.; McAdoo, D. J. Org Mass Spectrom 1989, 24, 866.

14. Dorgio, A. E.; McCarrick, M. A.; Loncharich, R. J.; Houk, K. N. J Am Chem Soc 1990, 112, 7508.
15. Trigueros, P. P.; Casanovas, J.; Alemán, C.; Vega, M. C. J Mol Struct (Theochem) 1992, 277, 117.
16. Whiteside, R. A.; Frisch, M. J.; Pople, J. A. The Carnegie-Mellon Quantum Chemistry Archive; Department of Chemistry, Carnegie-Mellon University: Pittsburgh, PA, 1983.
17. Henry, D. J.; Parkinson, J.; Mayer, P. M.; Radom, L. J Phys Chem A 2001, 105, 6750; and references therein.
18. Frisch, M. J.; Trucks, G. W.; Schlegel, H. B.; Scuseria, G. E.; Robb, M. A.; Cheeseman, J. R.; Montgomery, J. A., Jr.; Vreven, T.; Kudin, K. N.; Burant, J. C.; Millam, J. M.; Iyengar, S. S.; Tomasi, J.; Barone, V.; Mennucci, B.; Cossi, M.; Scalmani, G.; Rega, N.; Petersson, G. A.; Nakatsuji, H.; Hada, M.; Ehara, M.; Toyota, K.; Fukuda, R.; Hasegawa, J.; Ishida, M.; Nakajima, T.; Honda, Y.; Kitao, O.; Nakai, H.; Klene, M.; Li, X.; Knox, J. E.; Hratchian, H. P.; Cross, J. B.; Bakken, V.; Adamo, C.; Jaramillo, J.; Gomperts, R.; Stratmann, R. E.; Yazyev, O.; Austin, A. J.; Cammi, R.; Pomelli, C.; Ochterski, J. W.; Ayala, P. Y.; Morokuma, K.; Voth, G. A.; Salvador, P.; Dannenberg, J. J.; Zakrzewski, V. G.; Dapprich, S.; Daniels, A. D.; Strain, M. C.; Farkas, O.; Malick, D. K.; Rabuck, A. D.; Raghavachari, K.; Foresman, J. B.; Ortiz, J. V.; Cui, Q.; Baboul, A. G.; Clifford, S.; Cioslowski, J.; Stefanov, B. B.; Liu, G.; Liashenko, A.; Piskorz, P.; Komaromi, I.; Martin, R. L.; Fox, D. J.; Keith, T.; Al-Laham, M. A.; Peng, C. Y.; Nanayakkara, A.; Challacombe, M.; Gill, P. M. W.; Johnson, B.; Chen, W.; Wong, M. W.; Gonzalez, C.; Pople, J. A. Gaussian 03, Revision C.02; Gaussian, Inc.: Wallingford CT, 2004.
19. Flükiger, P.; Lüthi, H. P.; Portmann, S.; Weber, J. MOLEKEL-4.3; Swiss Center for Scientific Computing: Manno, Switzerland, 2000.
20. Zhao, Y.; González-García, N.; Truhlar, D. G. J Phys Chem A 2005, 109, 2012.
21. Alcamí, M.; Mó, O.; Yáñez, M. Mass Spectrom Rev 2001, 20, 195.
22. Batra, R.; Giese, B.; Spichty, M.; Gescheidt, G.; Houk, K. N. J Phys Chem 1996, 100, 18371.
23. Norberg, D.; Larsson, P.-E.; Dong, X.-C.; Salhi-Benachenhou, N.; Lunell, S. Int J Quantum Chem 2004, 98, 473.
24. Larsson, P.-E.; Salhi-Benachenhou, N.; Lunell, S. Chem Eur J 2004, 10, 681.
25. Norberg, D.; Larsson, P.-E.; Salhi-Benachenhou, N.; Lunell, S. Org Biomol Chem 2006, 4, 4241.
26. Besler, B. H.; Merz, K. M., Jr.; Kollman, P. A. J Comput Chem 1990, 11, 431.
27. Roohi, H; Ebrahimi, A. J Mol. Struct (Theochem) 2005, 726, 141; and references therein.
28. Davey, J. B.; Greenslade, M. E.; Marshall, M. D.; Lester, M. I.; Wheeler, M. D. J Chem Phys 2004, 121, 3009.
29. Selçuki, C.; Aviyente, V. J Mol Model 2001, 7, 398.
30. Belevskii, V. N.; Tyurin, D. A.; Chuvylkin, N. D. High Energy Chem 1998, 32, 381.